J|A|C|S
ARTICLES
Published on Web 06/28/2002

Combinations of Microphase Separation and Terminal Multiple Hydrogen Bonding in Novel Macromolecules

Koji Yamauchi,† Jeremy R. Lizotte,† David M. Hercules,‡ Matthew J. Vergne,‡ and Timothy E. Long*,†

Contribution from the Department of Chemistry and Polymeric Materials and Interfaces Laboratories, Virginia Polytechnic Institute and State University, Blacksburg, Virginia 24061-0212, and Department of Chemistry, Box 1822 Station B, Vanderbilt University, Nashville, Tennessee 37235

Received January 23, 2002

Abstract: The synthesis and characterization of terminal multiple hydrogen-bonded (*MHB*) polymers, such as poly(styrene) (PS), poly(isoprene) (PI), and microphase separated PS-*b*-PI block copolymers, possessing controlled molecular weights and narrow molecular distributions are described. Hydroxyl-terminated polymeric precursors were prepared using living anionic polymerization and subsequent quantitative termination with ethylene oxide. *MHB* polymers were synthesized in a controlled fashion via end-group modification of these well-defined macromolecular alcohols with excess isophorone diisocyanate and subsequent derivatization of the isocyanate-terminated polymeric intermediate with methyl isocytosine. The glass transition temperatures of the terminal *MHB* polymers were reproducibly higher than both nonfunctionalized and hydroxyl-terminated polymers at nearly equivalent number average molecular weights. Thin-layer chromatography analysis indicated that the interaction of terminal *MHB* polymers with silica was stronger as compared to both nonfunctionalized and hydroxyl-terminated polymers. Rheological characterization indicated that the melt viscosity at constant shear rate for various *MHB* polymers was more than 100 times higher than those for nonfunctionalized and hydroxyl-terminated polymers. Interestingly, the melt viscosity of *MHB* polymers was higher than those of nonfunctionalized polymers with twice the number average molecular weight. In addition, DSC and rheological characterization also suggested that terminal *MHB* polymers formed aggregates and not simple dimers in the melt state, and the aggregates were observed to completely dissociate at 80 °C.

Introduction

Synthetic methodologies for the preparation of high performance macromolecules have traditionally focused on macromolecules that are constructed using irreversible covalent bonding. However, noncovalent bonding, such as multiple hydrogen and ionic bonding, has recently received renewed significant attention.[1−13] Noncovalent bonding in macromolecules will result in new supramolecular structures that have unique combinations of thermal reversibility, melt processability, recyclability, interfacial adhesion, and enhanced compatibility in polymer blends. Meijer et al. recently reported the utility of multiple hydrogen bonding between 2-ureido-4[1H]-pyrimidone (UPy) units attached to a hexamethylene spacer,[14,15] *m*-xylylene spacer,[16] oligo(ethylene glycol),[14,17] oligo(ethylene glycol-*co*-propylene glycol) copolymer,[14,17] and poly(dimethylsiloxane).[14] These noncovalent bonded molecules resulted in polymer-like properties including shear thinning, viscoelastic behavior, and glass transition temperatures and were sufficiently strong to construct novel supramolecular architectures. Meijer also proposed that these multiple hydrogen-bonded molecules formed dimers in both solution and the solid state.[17−22]

---

* To whom correspondence should be addressed. E-mail: telong@vt.edu.
† Virginia Polytechnic Institute and State University.
‡ Vanderbilt University.

(1) Reinhoudt, D. N. *Supramolecular Materials and Technologies*; J. Wiley & Sons: New York, 1999; Vol. 4.
(2) Brunsveld, L.; Folmer, B. J. B.; Meijer, E. W.; Sijbesma, R. P. *Chem. Rev.* **2001**, *101*, 4071.
(3) Jeffrey, G. A. *An Introduction to Hydrogen Bonding*; Oxford University Press: New York, 1997.
(4) Vuillaume, P. Y.; Galin, J. C.; Bazuin, C. G. *Macromolecules* **2001**, *34*, 859.
(5) Samios, C. K.; Kalfoglou, N. K. *Polymer* **2001**, *42*, 3687.
(6) Kato, T.; Fréchet, J. M. J. *Macromol. Symp.* **1995**, *98*, 311.
(7) Kihara, H.; Kato, T.; Uryu, T.; Fréchet, J. M. J. *Chem. Mater.* **1996**, *8*, 961.
(8) Kato, T.; Kihara, H.; Ujiie, S.; Uryu, T.; Fréchet, J. M. J. *Macromolecules* **1996**, *29*, 8734.
(9) Xu, Z.; Kramer, E. J.; Edgecombe, B. D.; Fréchet, J. M. J. *Macromolecules* **1997**, *30*, 7958.
(10) Palacin, S.; Chin, N. D.; Simanek, E. E.; MacDonald, C. J.; Whitesides, G. M.; McBridge, T. M.; Palmore, R. T. *J. Am. Chem. Soc.* **1997**, *119*, 11807.
(11) Simanek, E. E.; Isaacs, L.; Wang, C. C. C.; Whitesides, G. M. *J. Org. Chem.* **1997**, *62*, 8994.
(12) Mammen, M.; Shakhnovich, I. E.; Deutch, M. J.; Whitesides, G. M. *J. Org. Chem.* **1998**, *63*, 3821.
(13) Choi, S. I.; Li, X.; Simanek, E. E.; Akaba, R.; Whitesides, G. M. *Chem. Mater.* **1999**, *11*, 684.
(14) Sijbesma, R. P.; Beijer, F. H.; Brunsveld, L.; Folmer, B. J. B.; Hirschberg, J. H. K. K.; Lange, R. F. M.; Lowe, J. K. L.; Meijer, E. W. *Science* **1997**, *278*, 1601.
(15) Folmer, B. J. B.; Sijbesma, R. P.; Meijer, E. W. *J. Am. Chem. Soc.* **2001**, *123*, 2093.
(16) Folmer, B. J. B.; Sijbesma, R. P.; Kooijman, H.; Spek, A. L.; Meijer, E. W. *J. Am. Chem. Soc.* **1999**, *121*, 9001.
(17) Lange, R. F. M.; Gurp, M.; Meijer, E. W. *J. Polym. Sci., Part A: Polym. Chem.* **1999**, *37*, 3657.

10.1021/ja020123e CCC: $22.00 © 2002 American Chemical Society

Jean-Marie Lehn et al. have also focused on the selective formation of discrete supramolecules from complementary receptor−substrate hydrogen bonding pairs. Molecular recognition induced aggregation, and fusion was reported between vesicles containing complementary lipids bearing bartituric acid and triaminopyrimidine units as headgroups through the formation of three hydrogen bonds.[23−26] Self-organized molecules consisting of alternating 2,6-diaminopyridine and 2,6-pyridinedicarbonyl units were prepared, and the helical conformation in the solid state was thoroughly characterized.[25,26]

Stadler et al. reported microphase separated poly(isoprene)-*block*-poly(1,3-butadiene) diblock copolymers with random hydrogen bonds based on phenylurazole.[27] It was shown that hydrogen bonding induced microphase separation in an originally miscible block copolymer and resulted in the formation of a thermoreversible network structure. Stadler also reported DSC, dielectric, and dynamic mechanical analysis of telechelic hydrogen-bonded poly(isobutylene) containing 4-urazoylbenzoic acid.[28] The melting temperature of the ordered aggregates ranged from 380 to 390 K using DSC analysis, and distortions were monitored below the melting temperature using dielectric mechanical measurements.

The versatility of "plug and play" polymers that are accessible using complementary hydrogen bonds was reported recently by Rotello et al. In particular, the synthesis of diaminotriazine-functionalized poly(styrene)s and molecular recognition of flavin as a guest molecule were reported.[29−31] Rotello has shown that the recognition efficiency between a polymer and guest is controllable through the judicious choice of recognition element and a tailored balance between intra- and intermolecular interactions.

Our current efforts have focused on the synthesis of well-defined terminal multiple hydrogen-bonded polymers, such as glassy poly(styrene) (PS), rubbery poly(isoprene) (PI), and microphase separated PS-*b*-PI block copolymers with well-defined molecular weights and narrow molecular weight distributions. The relationship between end-group structure and physical performance, such as thermal, rheological, and morphological properties, was investigated. We report herein the unprecedented synthesis of terminal multiple hydrogen-bonded block copolymers using living anionic polymerization to fundamentally understand the behavior of well-defined *MHB* polymers, especially aggregation state, dissociation temperature of the *MHB* polymers, and the potential synergy of microphase separation and noncovalent multiple hydrogen bonding.

Scheme 1. Reaction Scheme for End-Group Modification

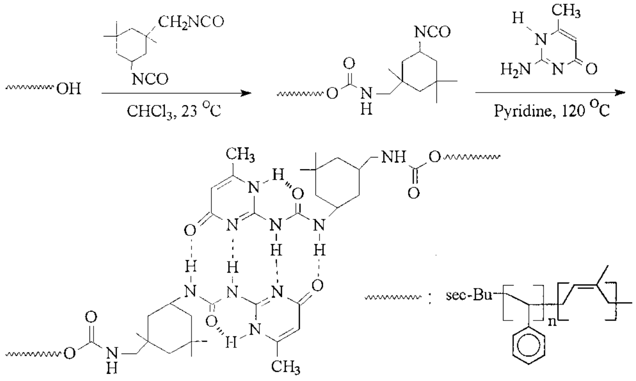

Results and Discussion

Synthesis of terminal multiple hydrogen-bonded (*MHB*) polymers involved a two-step synthesis; the first step involved the synthesis of well-defined hydroxyl-terminated polymers, which were synthesized via living anionic polymerization, followed by an end-capping reaction with EO. In the second step, terminal *MHB* polymers were synthesized via the end-group modification of well-defined hydroxyl-terminated polymers with an excess of IPDI and MIS to avoid undesirable coupling during functionalization (Scheme 1).

Synthesis of Nonfunctionalized PS (PSH) and Hydroxyl-Terminated PS (PSOH). Molecular weights and molecular weight distributions for PSH and PSOH are summarized in Table 1. The molecular weight distributions of PSH and PSOH were narrow ($M_w/M_n = 1.01-1.05$), and the theoretical molecular weights, which were calculated from the ratio of monomer to initiator ([M]/[I]), were in good agreement with the molecular weight measured using GPC and MALDI. On the basis of a comparison of ^{1}H NMR spectra for PSH and PSOH, the hydroxyl end-group ($-\mathrm{CH_2C}H_2\mathrm{OH}$) was assigned at 3.3−3.5 ppm, and the *sec*-butyl end-group ($\mathrm{CH_3CH_2CH(CH_3)_2}$) was assigned at 0.6−1.0 ppm. Number average molecular weights were calculated from the relative integrals associated with the repeating unit, such as the aromatic protons at 6.3−7.5 ppm with the methylene in the hydroxyl end-group ($-\mathrm{CH_2C}H_2\mathrm{OH}$) at 3.3−3.5 ppm or the *sec*-butyl end-group at 0.6−1.0 ppm. The number average molecular weights as estimated from ^{1}H NMR spectra were in good agreement with those obtained using GPC.

End-Group Modification of PSOH. *MHB* PS was synthesized via the further modification of PSOH with IPDI and MIS as shown in Scheme 1. Table 2 summarizes the molecular weights and molecular weight distributions of *MHB* PS that were obtained via end-group modification of PS-OH. A comparison of the ^{1}H NMR spectra for the precursor and corresponding reaction product revealed that the signal at 3.3−3.5 ppm, which was assigned to $-\mathrm{CH_2C}H_2\mathrm{OH}$, disappeared, and new resonances, such as $-\mathrm{CH_2C}H_2\mathrm{O}-$ (3.5−3.9 ppm), $-\mathrm{CH_2C}H_2\mathrm{NH}-$ (3.0−3.2 ppm), and $-\mathrm{C}H{=}\mathrm{C}-$ (5.8 ppm), appeared. In addition, three NH signals ($-\mathrm{CH_2N}H-\mathrm{CO}-$, $-\mathrm{CHN}H-\mathrm{CO}-\mathrm{NH}-$, 10.0 ppm (overlapped); $-\mathrm{N}H-\mathrm{C}{=}\mathrm{N}-$, 12.0 ppm; $-\mathrm{N}H-\mathrm{C(CH_3)}{=}$, 13.0 ppm) were observed. A comparison of FTIR spectra of PSOH-2 and the reaction product (*MHB* PS-2) revealed that a

---

(18) Hirschberg, J. H. K. K.; Beijer, F. H.; Aert, H. A.; Magusin, P. C. M. M.; Sijbesma, R. P.; Meijer, E. W. *Macromolecules* **1999**, *32*, 2696.

(19) Beijer, F. H.; Sijbesma, R. P.; Kooijman, H.; Spek, A. J.; Meijer, E. W. *J. Am. Chem. Soc.* **1998**, *120*, 6761.

(20) Söntjens, S. H. M.; Sijbesma, R. P.; Genderen, M. H. P.; Meijer, E. W. *J. Am. Chem. Soc.* **2000**, *122*, 7487.

(21) Söntjens, S. H. M.; Sijbesma, R. P.; Genderen, M. H. P.; Meijer, E. W. *Macromolecules* **2001**, *34*, 3815.

(22) Folmer, B. J. B.; Sijbesma, R. P.; Kooijmaan, H.; Spek, A. L.; Meijer, E. W. *J. Am. Chem. Soc.* **1999**, *121*, 9001.

(23) Artzner, V. M.; Jullien, L.; Gulik-Krzywicki, T.; Lehn. J.-M. *Chem. Commun.* **1997**, 117.

(24) Russel, K. C.; Lehn, J.-M.; Kyritsakas, N.; DeCian, A.; Fischer, J. *New J. Chem.* **1998**, *22(2)*, 123.

(25) Berl, V.; Huc, I.; Khoury, R. G.; Lehn, J.-M. *Chem.-Eur. J.* **2001**, *7(13)*, 2798.

(26) Berl, V.; Huc, I.; Khoury, R. G.; Lehn, J.-M. *Chem.-Eur. J.* **2001**, *7(13)*, 2810.

(27) Freitas, L. L.; Jacobi, M. M.; Gonçalves, G.; Stadler, R. *Macromolecules* **1998**, *31*, 3379.

(28) Müller, M.; Dardin, A.; Seidel, U.; Balsamo, V.; Iván, B.; Spiess, H. W.; Stadler, R. *Macromolecules* **1996**, *29*, 2577.

(29) Deans, R.; Ilhan, F.; Rotello, V. M. *Macromolecules* **1999**, *32*, 4956.

(30) Ilhan, F.; Galow, T. H.; Gray, M.; Clavier, G.; Rotello, V. M. *J. Am. Chem. Soc.* **2000**, *122*, 5895.

(31) Ilhan, F.; Gray, M.; Rotello, V. M. *Macromolecules* **2001**, *34*, 2597.

Table 1. Molecular Weights and Molecular Weight Distributions for PSH and PSOH

	SEC DRI		SEC MALLS		M_n[c]		MALDI		
sample[a]	M_n	M_W/M_n	M_n	M_W/M_n	estimated from *sec*-Bu	estimated from CH_2CH_2OH	M_n	M_W/M_n	T_g[d] (°C)
PSH-1	2500	1.07	2950	1.05	2900				65
PSH-2	4140	1.04	5240	1.02	4700		5380	1.03	75
PSH-3	9850	1.03	10 200	1.03	10 000				86
PSH-4	22 100	1.03	25 800	1.01	25 500				88
PSOH-1[b]	2400	1.05	2890	1.04	2400	2100	2620	1.08	72
PSOH-2	4700	1.04	5960	1.02	5700	5000	5050	1.03	84
PSOH-3	22 000	1.03	24 900	1.01	24 500	25 200			91

[a] 10 wt % monomer solution using *sec*-BuLi at 23 °C for 2 h. [b] EO in 10 times excess as compared to the initiator concentration was used for the end-capping reaction. [c] Estimated from 400 MHz ^1H NMR spectrum. [d] Measured by DSC, mid-point of the second heat.

Table 2. Molecular Weights and Molecular Weight Distributions for *MHB* PS

	SEC DRI		SEC MALLS		M_n[b]		MALDI		
sample[a]	M_n	M_W/M_n	M_n	M_W/M_n	estimated from *sec*-Bu	estimated from *MHB* unit[c]	M_n	M_W/M_n	T_g[d] (°C)
MHB PS-1	2790	1.05	3320	1.04	2800	2400	2880	1.04	92
MHB PS-2	4840	1.04	5700	1.03	5200	5200	5180	1.03	92
MHB PS-3	22 200	1.04	30 900	1.03	31 800	30 000			99

[a] PSOH was reacted with 1.2 times excess of IPDI as compared to hydroxyl in $CHCl_3$ at 25 °C/24 h, evaporated, followed by reaction with 21 times excess of MIS as compared to hydroxyl at 150 °C/24 h. [b] Estimated from 400 MHz ^1H NMR. [c] Calculated from the relative intensities of reasonances associated with the repeating units such as $-C_6H_5$, $-NH-$, $-C{=}CH-$, $-CH_2NH-$, $-CH_2OCO-$. [d] Measured by DSC, mid-point of the second heat.

Table 3. Molecular Weights and Molecular Weight Distributions of PIH, PIOH, and *MHB* PI

	SEC DRI		SEC MALLS		M_n[b]		
sample[a]	M_n	M_W/M_n	M_n	M_W/M_n	estimated from *sec*-Bu	estimated from MHB unit[c]	T_g[d] (°C)
PIH-1	4710	1.05	3430	1.02	2500		−68
PIOH-1	3960	1.10	3050	1.08	2600	2600	−65
MHB PI-1	4090	1.07	3780	1.12	3300	3400	−61
PIH-2	6670	1.04	5700	1.02	5500		−67
PIOH-2	7220	1.11	6790	1.12	5200	5600	−62
MHB PI-2	7450	1.12	6850	1.25	5800	6200	−61
PIH-3	31 500	1.02	21 200	1.01	22 300		−66
PIOH-3	31 600	1.02	20 900	1.01	21 500	21 000	−65
MHB PI-3	30 900	1.03	22 700	1.02	23 000	21 500	−61
PIH-4	12 900	1.03	9300	1.02	9500		−66

[a] 10 wt % monomer solution using *sec*-BuLi at 23 °C for 2 h. [b] Estimated from 400 MHz ^1H NMR. [c] Calculated from the relative intensities of reasonances associated with the repeating units such as $-C_6H_5$, $-NH-$, $-C{=}CH-$, $-CH_2NH-$, $-CH_2OCO-$. [d] Measured by DSC, mid-point of the second heat.

new peak at 1720 cm^{-1}, which was assigned to $-NH-C({=}O)-O-$, and a second peak at 1680 cm^{-1}, which was assigned to $-NH-C({=}O)-NH-$, were observed after end-group modification.

A comparison of molecular weight data for precursors and the reaction products are summarized in Tables 1 and 2. GPC confirmed that molecular weights did not appreciably change upon end-group modification. In addition, number average molecular weights that were calculated from the integration ratio of phenyl ($CH{=}$) at 6.3−7.5 ppm and methylene in $-CH_2CH_2-NH-$ (3.0−3.2 ppm), $-CH_2CH_2O-$ (3.5−3.9 ppm), three NH signals ($-CH_2NH-CO-$, $-CHNH-CO-NH-$, 10.0 ppm (overlapped); $-NH-C{=}N-$, 12.0 ppm; $-NH-C(CH_3){=}$, 13.0 ppm), and *sec*-butyl (0.6−1.0 ppm) were in good agreement with GPC values.

Thin-layer chromatography (TLC) in different solvents such as chloroform, THF, and ethyl acetate did not detect either the PS-H homopolymer or the PSOH precursor. Therefore, end-group modification proceeded in a quantitative yield. TLC is a simple method to examine the interaction of a polymer with silica. In chloroform, PSH moved to the top of the plate; however, the interaction of PSOH with silica was stronger than that of PSH presumably because of the interaction of the hydroxyl end-group with silica. *MHB* PS did not transcend the TLC plate in chloroform. This suggested that the interaction of *MHB* polymer with silica was stronger than that of PSH and PSOH in chloroform. In a polar solvent, such as THF or ethyl acetate, all polymers moved to the top of the plate, indicating that *MHB* PS did not interact with silica in the presence of a polar solvent. Thus, end-group modification proceeded in a quantitative yield in the absence of undesirable side reactions. In addition, GPC measurements in THF at 40 °C suggested complete dissociation at typical analysis concentrations (1 mg/1 mL).

Molecular weights and molecular weight distributions for PI with various end-groups are summarized in Table 3. The molecular weight distributions of PIH and PIOH were narrow ($M_w/M_n = 1.01-1.12$), and the calculated molecular weights were in good agreement with molecular weights measured using GPC with MALLS. On the basis of a comparison of the ^1H NMR spectra of PIOH and *MHB* PI, the signal at 3.5−3.7 ppm, which was assigned to $-CH_2CH_2OH$, disappeared, and a

Table 4. Molecular Weights and Molecular Weight Distributions of PS-*b*-PI-H, PS-*b*-PI-OH, *MHB*-PS-*b*-PI, and PS-*b*-PI-*b*-PS Block Copolymers

	SEC DRI		SEC MALLS		M_n[b]			
sample[a]	M_n	M_w/M_n	M_n	M_w/M_n	estimated from *sec*-Bu	estimated from *MHB* unit[c]	[St]:[IP][b]	T_g[c,d] (°C)
PS-*b*-PI-H1	9900	1.03	8290	1.01	8100		25.7:74.3	−56
PS-*b*-PI-OH1	9150	1.10	8780	1.03	8300	8500	25.6:74.4	−52
MHB PS-*b*-PI1	9740	1.07	8400	1.03	8500	8500	25.6:74.4	−47
PS-*b*-PI-*b*-PS1	16 200	1.04	12 800	1.03	12 400		26.1:73.9	−57
PS-*b*-PI-H2	68 200	1.05	59 400	1.04	56 200		42.3:57.7	−57
PS-*b*-PI-OH2	60 500	1.03	46 900	1.02	45 200	41 500	40.1:59.9	−60
MHB PS-*b*-PI2	50 600	1.10	52 900	1.07	48 300	50 200	40.1:59.9	−60
PS-*b*-PI-*b*-PS2	150 000	1.04	101 000	1.09	117 900		40.1:59.9	−60

[a] 10 wt % monomer solution using *sec*-BuLi at 23 °C for 2 h. [b] Estimated from 400 MHz ^{1}H NMR spectrum. [c] Calculated from the relative intensities of reasonances associated with the repeating units such as $-C_6H_5$, $-NH-$, $-C{=}CH-$, $-CH_2NH-$, $-CH_2OCO-$. [d] Measured by DSC, mid-point of the second heat. [e] T_g of PS was not detected.

resonance assigned to the *MHB* unit appeared. The number average molecular weight did not appreciably change after end-group modification. Consequently, end-group modification proceeded in a quantitative manner. In addition, GPC analysis of *MHB* PI in THF suggested that *MHB* PI completely dissociated in THF at GPC analysis concentrations (1 mg/1 mL).

Synthesis of Nonfunctionalized, Hydroxyl, and *MHB* PS-*b*-PI Block Copolymers. Nonfunctionalized (PS-*b*-PI-H), hydroxyl-terminated (PS-*b*-PI-OH), and *MHB* PS-*b*-PI block copolymers were synthesized using methodologies similar to those of PS and PI. PS-*b*-PI-*b*-PS triblock copolymers (PS-*b*-PI-*b*-PS) were also synthesized to ascertain the end-group effect on rheological and morphological properties.

Table 4 summarizes PS-*b*-PI block copolymers with three types of end-groups and comparative triblock copolymers. The molecular weight distributions were narrow ($M_w/M_n = 1.01-1.09$), and the calculated molecular weights were similar to the molecular weights measured using GPC with MALLS detection and ^{1}H NMR. The resonance for the hydroxyl end-group ($-CH_2CH_2OH$) was observed at 3.5−3.7 ppm in ^{1}H NMR spectra of PS-*b*-PI-OH. These spectra indicated that the $-CH_2CH_2OH$ signal at 3.5−3.7 ppm disappeared, and resonances assigned to the *MHB* unit were observed. In addition, number average molecular weights were calculated from the integrations of resonances associated with the repeating unit such as aromatic protons ($CH{=}$) at 6.3−7.5 ppm as compared to the methylene in $-CH_2CH_2NH-$ (3.0−3.2 ppm), $-CH_2CH_2O-$ (3.5−3.9 ppm), three NH signals (10.0 ppm ($-CH_2NH-CO-$, $-CHNH-CO-NH-$ (overlapped)), 12.0 ppm ($-NH-C{=}N-$), 13.0 ppm ($-NH-C(CH_3){=}$)), or *sec*-butyl (0.6−1.0 ppm). The number average molecular weight values all agreed within experimental error. Therefore, it was concluded that end-group modification proceeded in a quantitative fashion. The molecular weights measured by GPC did not appreciably change upon end-group modification as shown in Table 4.

Thermogravimetric Analysis. Figure 1 depicts thermogravimetric analysis (TGA) of *MHB* PS. TGA data indicated that *MHB* PS exhibited an onset of weight loss at 200 °C, and the mechanism appeared to involve two steps. The first degradation step corresponded to the elimination of the multiple hydrogen-bonded end-group because the weight loss of the first step was similar to the theoretical weight of the *MHB* unit. PSOH was not as thermally stable as PSH presumably because of dehydration of the hydroxyl ethyl end-group followed by degradation.

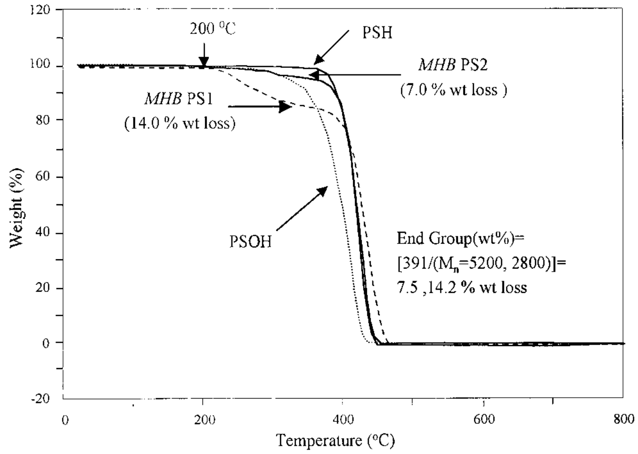

Figure 1. Thermogravimetric analysis of PS (PSH-1, PSOH-1, *MHB* PS-1, 2).

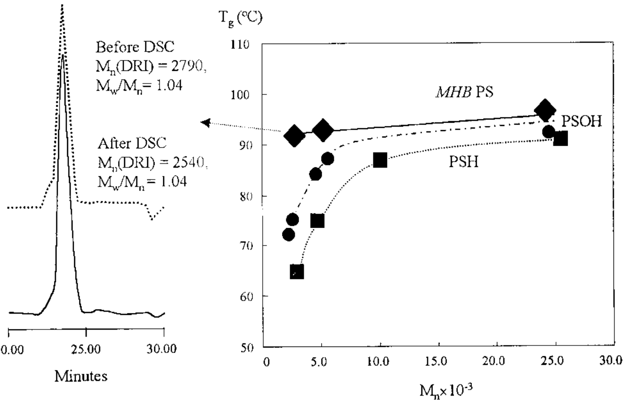

Figure 2. Relationship between M_n and T_g (DSC measured from 30 to 180 °C, 10 °C/min) and DSC curve of *MHB* PS1 (Waters SEC with external 410 RI detector, THF at 40 °C and 1.0 mL/min using polystyrene standards).

Glass Transition Temperature (T_g). Figure 2 illustrates the relationship between the number average molecular weight (M_n) and T_g. As expected, the T_g of PSH and PSOH increased as the molecular weight increased. Interestingly, at lower molecular weights, the T_g of *MHB* PS was much higher than that of PSOH, and the maximum T_g at lower molecular weights was observed. Molecular weight changes during the DSC measurement may affect the T_g; however, Figure 2 also confirmed that molecular weight did not change during the DSC measurement. This indicated that the higher T_g of *MHB* PS was because of the strong interaction among *MHB* units. If *MHB* PS aggregated as a simple dimer as described in the earlier literature,[17,20−22]

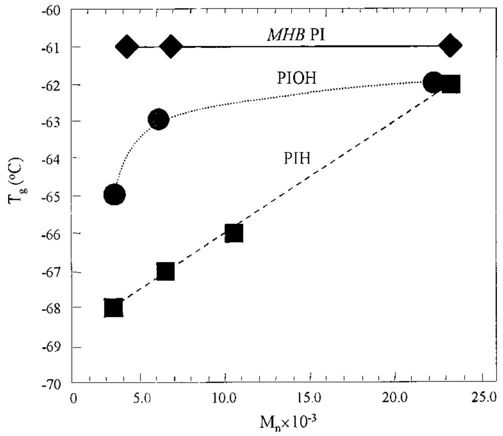

Figure 3. Relationship between M_n and T_g (DSC measured from −100 to 30 °C, 10 °C/min).

the *MHB* PS would exhibit a T_g similar to that of PSH with twice the molecular weight. However, the T_g of *MHB* PS-1 (M_n = 2800, determined using ^{1}H NMR) was much higher than that of PSH-3 (M_n = 10 000). The relationship between molecular weight and T_g suggested that *MHB* polymers formed aggregates in a multiple fashion in the melt state. However, because of the possible proximity of the poly(styrene) glass transition temperature with the hydrogen bond dissociation temperature, functionalized poly(isoprenes) which have substantially lower glass transition temperatures (−60 °C) were investigated.

The relationship between M_n and T_g of PI is shown in Figure 3. As observed for PS, the T_g of *MHB* PI indicated a maximum value at lower molecular weight and was much higher than PIH and PIOH. The T_g of *MHB* PI-1 (M_n = 3300) or *MHB* PI-2 (M_n = 5800) was higher than that of PIH-2 (M_n = 5500) or PIH-3 (M_n = 22 300). This suggested that *MHB* polymers also aggregated in the bulk state. Meijer reported that multiple hydrogen-bonded molecules exhibited glass transition temperatures as evidence of polymer-like properties.[14] However, earlier reports did not discuss the effect of *MHB* end-groups on the glass transition temperatures for narrow molecular weight distribution oligomers and polymers. DSC analysis clarified the relationship between number average molecular weights and T_g for well-defined *MHB* polymers and suggested the presence of multiple aggregates in the melt state.

Rheological Characterization. To more fully understand the association of *MHB* polymers in the melt state, rheological analysis of PIH-2, PIOH-2, and *MHB* PI-2 was performed, and the results are depicted in Figure 4. The melt viscosity of *MHB* PI-2 (M_n = 5800, determined using ^{1}H NMR) was 100 times higher than that of PIH-2 (M_n = 5500) and PIOH-2 (M_n = 5200). In addition, *MHB* PI-2 was much higher than PIH-4 (M_n = 9500).

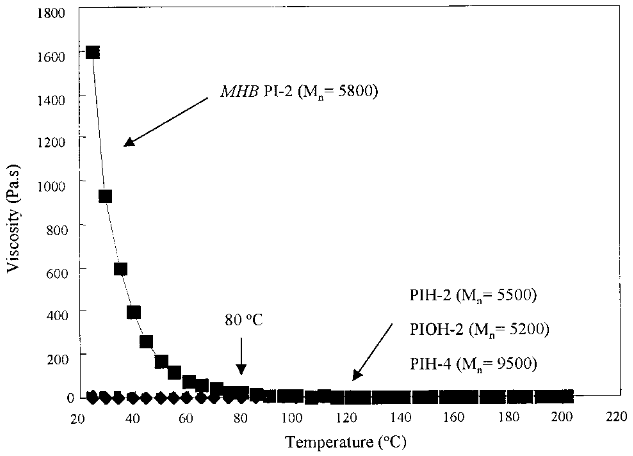

Figure 4. Effect of the end-group structure on the melt viscosity: rheological characterization of PIH-2, PIOH-2, and *MHB* PI-2 (temperature 150−180 °C, shear rate = 13.16 s^{-1}, a parallel plate fixture with the plate diameter = 25.0 mm and gap length = 1000 μm).

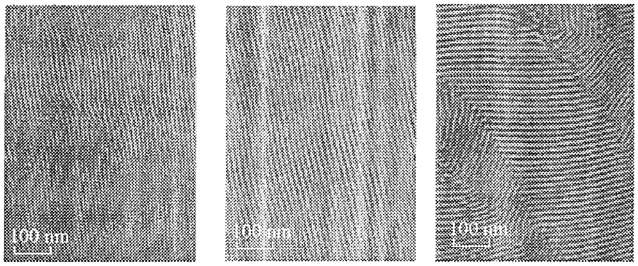

PS-b-PI-H2 M$_n$= 56200 PS-b-PI-OH2 M$_n$= 45200 *MHB* PS-b-PI2 M$_n$= 48300

Figure 5. TEM micrographs of PS-*b*-PI-H2 (M_n = 56 200) (left), PS-*b*-PI-OH2 (M_n = 45 200) (center), and *MHB* PS-*b*-PI2 (M_n = 4830) (right). The magnification is 172 500.

These data also suggested that *MHB* polymers formed aggregates in a multiple fashion in the melt state, which was consistent with DSC measurements. The melt viscosity of *MHB* PI approached PI-H and PI-OH at 80 °C, and dissociation of the multiple aggregates was confirmed at 80 °C. Rheological characterization of the PS-*b*-PI block copolymer with three different end-groups (PS-*b*-PI-H1, PS-*b*-PI-OH1, *MHB* PS-*b*-PI1) and comparative nonfunctionalized triblock copolymer (PS-*b*-PI-*b*-PI1) was also investigated. As observed for PI, the melt viscosity of *MHB* PS-*b*-PI1 (M_n = 8500) was more than 100 times higher than that of PS-*b*-PI-H1 (M_n = 8100) and PI-*b*-PS-OH1 (M_n = 8300) possibly because of the aggregation of *MHB* end-groups. In addition, *MHB* PS-*b*-PI1 was much higher than PS-*b*-PI-*b*-PS1 (M_n = 12 400) having a structure similar to that of a hypothetical PS-*b*-PI-H1 dimer. In addition, the melt viscosity of *MHB* PS-*b*-PI1 approached PS-*b*-PI-H1 and PS-*b*-PI-OH1 above 80 °C, and dissociation of the multiple aggregates was confirmed at 80 °C as observed for *MHB* PI. An understanding of the relationship between number average molecular weight for narrow molecular weight distribution samples and melt viscosity confirmed the multiple aggregation of the *MHB* functionalized polymers in the melt state.

Morphological Characterization. TEM micrographs of PS-*b*-PI block copolymers possessing three end-group types are shown in Figure 5. A well-defined lamellar structure consisting of PI (black) and PS (white) was observed in PS-*b*-PI-H, PS-*b*-PI-OH, and *MHB* PS-*b*-PI. In addition, hydroxyl and *MHB* termination did not significantly affect the morphology of PS-*b*-PI having high molecular weights in the spinodal composition ([St]:[IP] = 40:60 mol %) range. It is proposed that the *MHB* did not appreciably affect the morphology because of low end-group concentrations at high number average molecular weights (>45 000) that are required for film formation. The effect of block copolymer composition and block molecular weights on the resulting microphase separated morphologies will be addressed in detail in a future publication.

Conclusions

Terminal *MHB* polymers were synthesized via living anionic polymerization and end-group modification of well-defined hydroxyl-terminated polymers. Hydroxyl-terminated PS, PI, and PS-*b*-PI block copolymer as precursors were prepared using living anionic polymerization in the presence of *sec*-BuLi and subsequent quantitative termination with EO. Terminal *MHB* polymers were synthesized in a controlled fashion via end-group modification of these well-defined hydroxyl-terminated polymers with excesses of IPDI and subsequent derivatization of the isocyanate-terminated polymeric intermediate with MIS. The T_g of *MHB* polymers was reproducibly higher than both nonfunctionalized and hydroxyl-terminated polymers at nearly equivalent number average molecular weights. TLC analysis indicated that the interaction of *MHB* polymers with silica was stronger as compared to both nonfunctionalized and hydroxyl-terminated polymers. Thermogravimetric analysis of *MHB* polymers exhibited an onset of weight loss at 200 °C. Rheological characterization indicated that the melt viscosity at constant shear rate of terminal *MHB* polymers was more than 100 times higher than those of nonfunctionalized and hydroxyl-terminated polymers. Intriguingly, the melt viscosity of *MHB* polymers was higher than those of nonfunctionalized polymers with twice the number average molecular weight. DSC and rheological characterization suggested that terminal *MHB* polymers formed multiple aggregates and not simple dimers in the melt state as reported in earlier literature. On the basis of the rheological characterization, complete dissociation of the aggregates was confirmed at 80 °C. TEM micrographs of PS-*b*-PI block copolymers exhibited a well-defined lamellar structure; however, *MHB* termination did not appreciably affect the morphology in the spinodal composition range. The effect of copolymer composition and block molecular weights on the resulting morphology will be addressed in detail in a future publication.

Acknowledgment. The authors of this paper would like to thank Prof. David Hercules and Matthew Vergne at Vanderbilt University for MALDI experiments. The authors would like to thank A. J. Pasquale for GPC measurements, Victoria K. Long and Nicholas A. Gariano for rheological measurements, Phillip H. Madison for DSC measurements, and Mr. Stephen McCartney in the Department of Chemical Engineering for TEM analysis. We also thank TORAY Industries, Inc., Jeffress Memorial Trust, National Science Foundation (NSF CRIF 9974632). and Petroleum Research Fund (35190-AC7) for financial support.

Supporting Information Available: Experimental section, reaction scheme for synthesis of well-defined hydroxyl-terminated polymers (PI, PS, PS-*b*-PI block copolymer) (Scheme S1), reaction scheme for synthesis of nonfunctionalized, hydroxyl-terminated PS-*b*-PI block copolymer (Scheme S2), ^{1}H NMR spectra of PSOH-2 and the reaction product (*MHB* PS2) (Figure S1), GPC trace of PSOH-2 and the reaction product (*MHB* PS-2) (Figure S2), ^{1}H NMR spectra of PIOH-2 and the reaction product (*MHB* PI-2) (Figure S3), GPC trace of PIOH-2 and the reaction product (*MHB* PI-2) (Figure S4), rheological characterization of PIH-2, PIOH-2, and *MHB* PI-2 (Figure S5), rheological characterization of PS-*b*-PI-H, PS-*b*-PI-OH, and *MHB* PS-*b*-PI (Figures S6, S7) (PDF). This material is available free of charge via the Internet at http://pubs.acs.org.

JA020123E